Characterization of soil hydraulic properties heterogeneity in sandy soil by tomographic analysis and particle size distribution.

Yann Periard (1), Silvio José Gumiere (1), Alain N. Rousseau (2), Jonathan A. Lafond (1) and Jean Caron (1)

yann.periard-larrivee.1@ulaval.ca

(1) Université Laval, Faculté des sciences de l'agriculture et de l'alimentation, Département des sols et de génie agroalimentaire, Québec, Canada ,

(2) Institut national de la recherche scientifique : Centre Eau Terre Environnement (INRS-ETE), Québec, Canada, QC

Synergy in Science: Partnering for Solutions
ASA•CSSA•SSSA 2015 MEETING
November 15-18
Minneapolis, MN

Session: Hydrogeology, Environmental Soil Physics and Hydrology Student Competition: Lightning Orals with Posters: II - Poster Board Number: 1523

Introduction

- Knowledge about soil hydraulic properties are fundamental
- Characterization of these properties is very time-consuming
- Tomography imagery allow characterization of a number of soil hydraulic properties (Wildenschild and Sheppard, 2013)
- µCT-scan is limited to very small sample, which is inappropriate to study a representative volume of soil (soil profiles).

Objective

- The main objective of this work is to propose a framework to predict soil hydraulic properties from the combination of particle size distribution with X-ray tomography of a porous media.

Materials & Methods

1. Soils characterization

- Soil sample contained in a 15-cm long, 5-cm wide cylinder
- Unconsolidated Ottawa sand
- Curves of water retention and hydraulic conductivity obtained using the instantaneous profile method

2. Particle distribution

- Particle size distribution = LA950v2 Laser Particle Size Analyzer (Horiba)
- *n*th moment

$$m_n = \exp\left(n\mu_y + \frac{n^2\sigma^2}{2}\right)$$

- Cumulative mass fraction

$$M(R) = W\left(1-\frac{1}{2}erfc\left(\frac{\ln R-(\mu_y+3\sigma_y^2)}{\sqrt{2}\sigma_y}\right)\right) + (1-W)\left(1-\frac{1}{2}erfc\left(\frac{\ln R-(\mu_{2y}+3\sigma_{2y}^2)}{\sqrt{2}\sigma_{2y}}\right)\right)$$

- μ_y = mean of ln R
- σ_y = standard deviation of ln R
- W = weighting factor for the *i*th sub-distribution

3. Tomographic analysis

- Scans were performed at *Laboratoire Multidisplinaire de Scanographie du Québec de l'INRS-ETE.*
- Type of Medical CT scan : Somatum Volume Access (Siemens, Oakville, ON, CA).
- Energy level of 140, 120, 100 and 80 keV
- Voxel resolution of 0.1x0.1x0.6 mm

Figure 1. Medical CT scan

Materials & methods

4. Determination of the porosity

- Hounsfield scale
- Hu = attenuation coefficient of the soil
- Hu_{quartz} = attenuation coefficient of quartz
- Hu_{air} = attenuation coefficient of air

Lambert-Beer law

$$I = I_0 \exp(-\mu x) \qquad HU = 1000(\mu-\mu_w)/(\mu_w-\mu_a)$$

$$\phi = \frac{Hu_{quartz}-Hu}{Hu_{quartz}-Hu_{air}}$$

5. Derivation of soil hydraulic properties

- Carnahan–Starling approximation of void nearest-surface complementary cummulative density function (Chan and Govindaraju, 2004)

$$e_{vn}(\delta) = (1-\eta)\exp\left\{-\eta S\left[a_0\left(\frac{\delta}{m_1}\right)^3 + a_1\left(\frac{\delta}{m_1}\right)^2 + a_2\left(\frac{\delta}{m_1}\right)\right]\right\}$$

where

$$S = \frac{m_1 m_2}{m_3}$$

$$a_0 = \frac{(m_1^2/m_2)(1-\eta)(1-\eta+3\eta S)+2\eta^2S^2}{(1-\eta)^3}$$

$$a_1 = \frac{6(m_1^2/m_2)(1-\eta)+9\eta S}{2(1-\eta)^2} \qquad a_2 = \frac{3}{1-\eta}$$

- Coefficients a_0, a_1, a_2 $\quad \eta = 1-\phi$
- S = surface ratio
- η = dimensionless reduced density

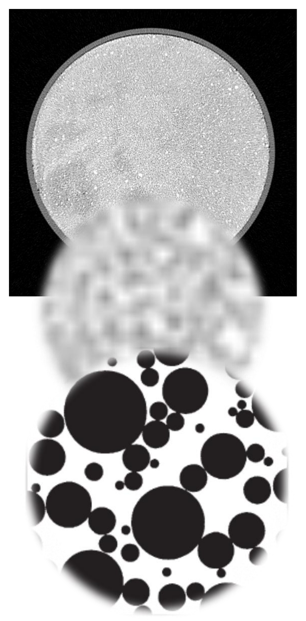

Figure 2. Polydisperse impenetrable hard spheres systems in 2D (Chan and Govindaraju, 2004)

- Nearest solid surface

$$\delta = ae^{br} \qquad r = \frac{2\sigma\cos\Psi}{\rho g h}$$

- Coefficients a, b
- σ = interfacial tension
- Ψ = contact angle
- g = gravitational acceleration
- ρ = density of the fluid
- h = soil matric potential

- Effective saturation

$$S_e = W\left(1-\frac{e_{v1}}{\phi}\right)+(1-W)\left(1-\frac{e_{v2}}{\phi}\right)$$

- Relative hydraulic conductivity (Mualem, 1976)

$$Kr = S_e^{\tau}\left(W\left(\frac{\int_0^{S_{e1}}\frac{1}{\psi(S_{e1})}dS_{e1}}{\int_0^{w}\frac{1}{\psi(S_{e1})}dS_{e1}}\right)+(1-W)\left(\frac{\int_0^{S_{e2}}\frac{1}{\psi(S_{e2})}dS_{e2}}{\int_0^{1-w}\frac{1}{\psi(S_{e2})}dS_{e2}}\right)\right)$$

- Saturated hydraulic conductivity (Nasta et al., (2013))

$$Ks = 3600\left(\frac{\rho_w g}{8\eta_w}\left(\frac{1}{\tau}\right)^2\int_0^{R_{max}}\frac{dS_e}{dr}r^2dr\right)$$

$$\frac{\partial^3 S_e}{\partial r^3} = 0 \quad and \quad \frac{\partial^2 S_e}{\partial r^2} < 0$$

Ghezzehei et al. (2007)

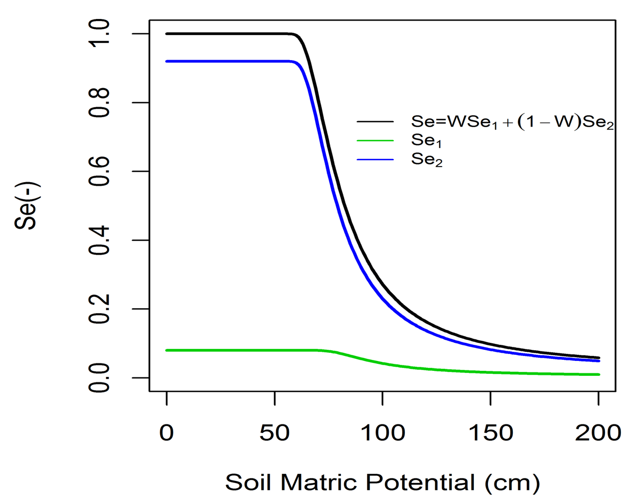

Figure 3. Dual model of effective saturation

6. Pore connectivity and tortuosity

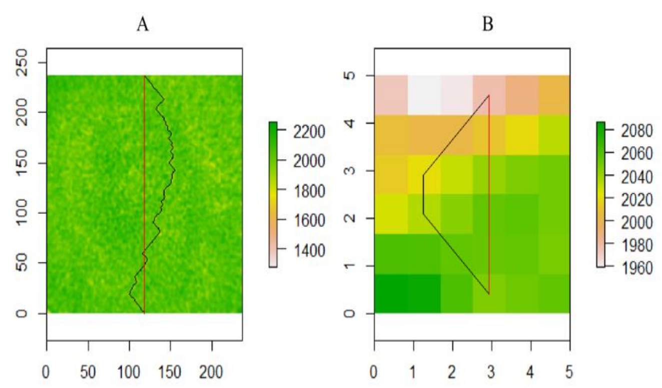

Figure 4. Simulation of water path from an image obtained with the CT scan. The Red line is the straight-line water path (L) and black line is the tortuous water path (Le). A is the water path from the image slice and B is a zoom in this water path

$$\tau = \frac{Le}{L}$$

$$Le = \sum_{i=1}^{n}\sqrt{(x_j-x_i)^2+(y_j-y_i)^2}$$

7. Computations

- Calcul Quebec http://www.calculquebec.ca
- Colosse supercomputer
- parallel implementation of R code
- Snow and RMPI library

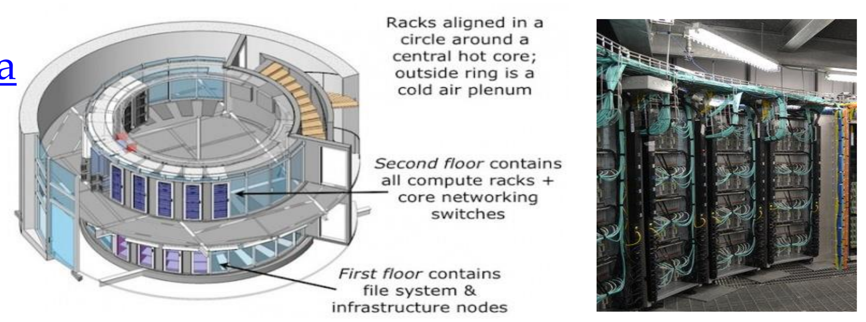

Figure 5. Colosse supercomputer

Results

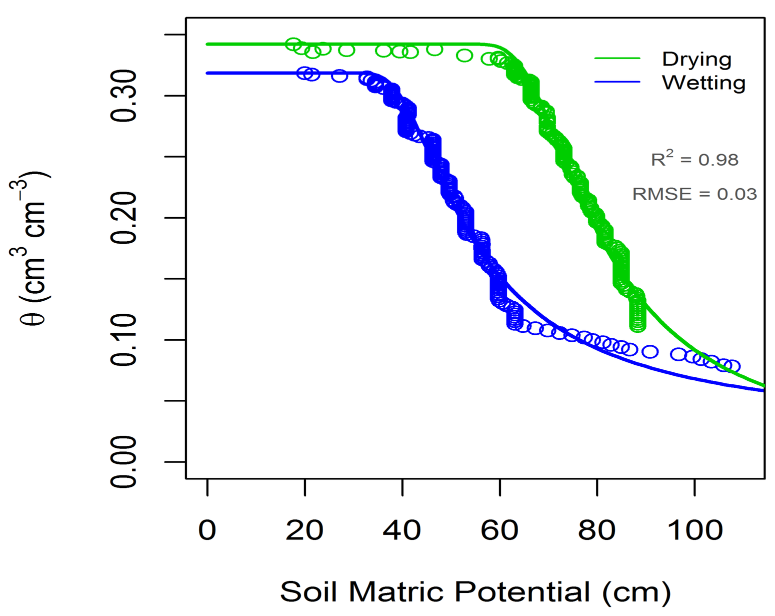

Figure 6. Soil water retention curves

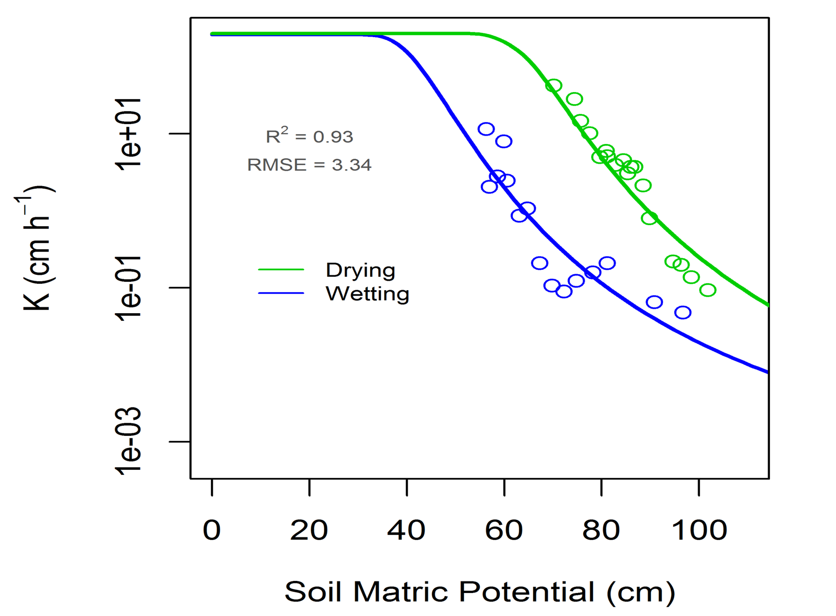

Figure 7. Soil hydraulic conductivity curves

- Good performance of the models to predict soil hydraulic properties (Figures 6 & 7)

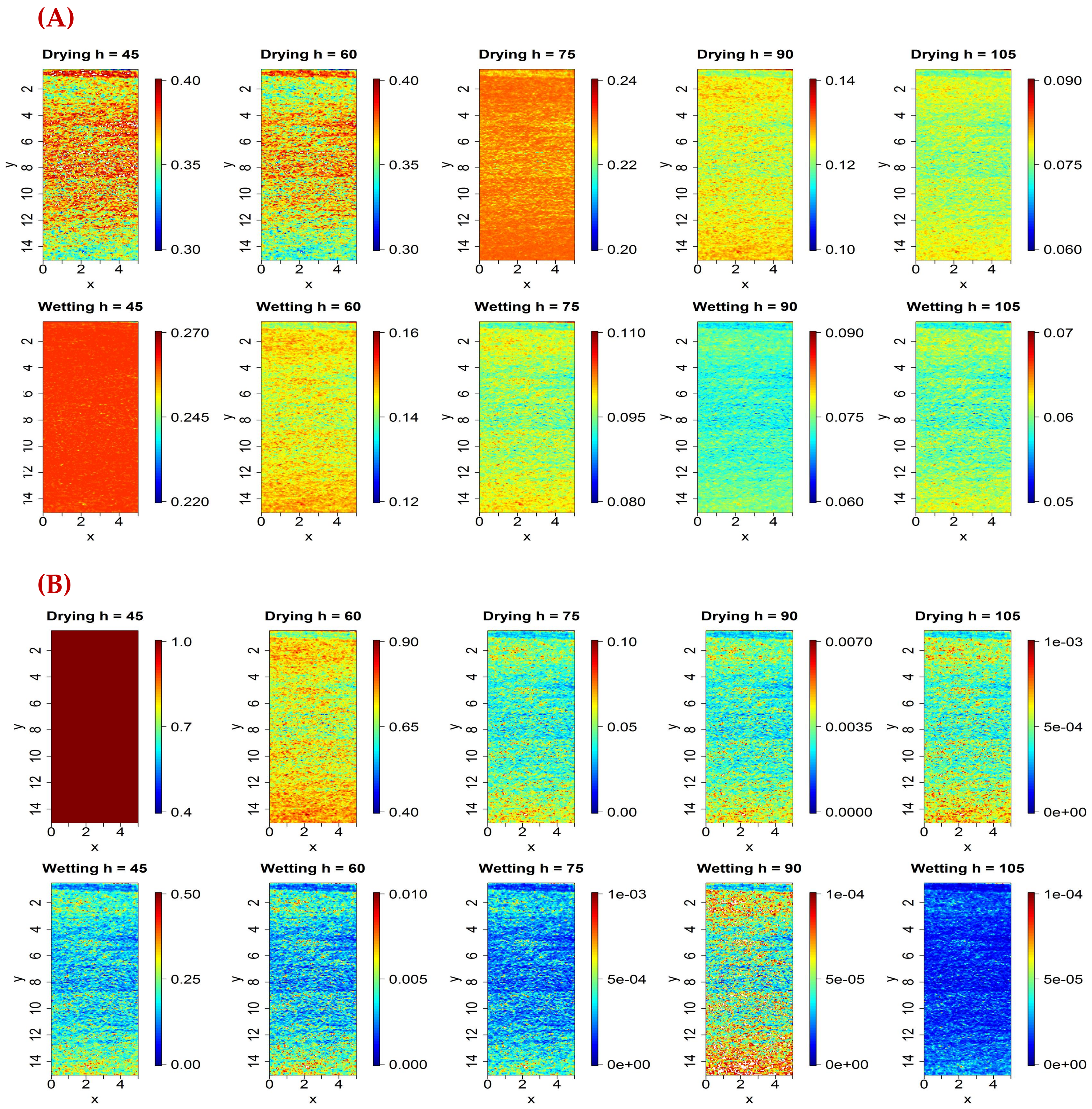

Figure 8. Radial plane of soil water content (A) and relative hydraulic conductivity (B) as a function of soil matric potential (h).

- High variability of soil hydraulic properties (Figure 8)
- Specifically in position of the curve with high variation of water content and relative hydraulic conductivity according to the matric potential (h).

Conclusion

- Using and analyzing Medical CT scans clearly show the variability of soil hydraulic properties in the sample.
- The framework provides a good prediction of the mean soil hydraulic properties.
- The framework provides an opportunity to study the variability of soil hydraulic properties over a monolith.

References

Chan, T.P., and R.S. Govindaraju. 2004. Estimating soil water retention curve from particle-size distribution data based on polydisperse sphere systems. *Vadose Zone J*. **3**:1443–1454.

Ghezzehei, T.A., T.J. Kneafsey & G.W. Su. (2007). Correspondence of the Gardner and van Genuchten–Mualem relative permeability function parameters. Water Resources Research 43: n/a-n/a. doi:10.1029/2006WR005339.

Nasta, P., J.A. Vrugt & N. Romano. (2013). Prediction of the saturated hydraulic conductivity from Brooks and Corey's water retention parameters. Water Resources Research 49: 2918-2925. doi:10.1002/wrcr.20269.

Wildenschild, D. and A.P. Sheppard. 2013. X-ray imaging and analysis techniques for quantifying pore-scale structure and processes in subsurface porous medium systems. Advances in Water Resources 51: 217-246. doi:http://dx.doi.org/10.1016/j.advwatres.2012.07.018.

Acknowledgements

NSERC CRSNG
Fonds de recherche sur la nature et les technologies Québec
ATOKA
Université Laval
Fruit d'Or
HORTAU